Excited State of the F Center in KI†

Kwangjai Park*

Department of Physics, University of California, Berkeley, California

(Received 7 July 1965)

The excited state (here called F^*) of the F center in KI was studied using a ruby laser as an excitation source. The absorption spectrum of the crystal was measured immediately before, during, and after an excitation pulse by using an auxiliary light source and monochromator. From these data the absorption spectra of the F^* center and the F' center were obtained. The fraction of the total number of centers maintained as F^* centers by the excitation pulse and the $F \to F'$ conversion during the pulse are interpreted in terms of a kinetic model which contains an important additional term beyond those in the usual models. The new term is due to the overlap between the strong absorption of the F^* and the ordinary fluorescence of the F^*. A nonradiative process ($2F^* \to F$+electron+vacancy), which can now take place in addition to the ordinary fluorescence, severely limits the population of F^* which can be maintained. The kinetics have been studied as a function of F-center concentration and laser intensity.

INTRODUCTION

THE optical absorption associated with the transition from the ground state to the first excited state of the F center has been the subject of extensive study for many years.[1,2] Recently there have been a number of experimental and theoretical activities to further understand the first excited state and the higher excited states of the F center. Through a careful and systematic study of the absorption spectra of several alkali halides, Lüty has established that the K and three L bands are due to the F center itself.[3] Although these bands are believed to rise from the transitions between the ground state and the higher excited states, much work is needed to arrive at a definitive conclusion regarding the origin of these bands.

An experiment which strongly motivated the present research is the recent work of Swank and Brown.[4] They measured the radiative lifetime of the relaxed first excited state (the F^*), and found it to be of the order of 10^{-6} sec. In view of this long lifetime, we can populate the first excited state using a high-intensity excitation source, and then use optical spectroscopy to examine the electrons in this state. The spectrum thus obtained should show the effect of depopulating the ground state as well as a continuum state and possibly other discrete states accessible from the first excited state.

The following sections contain a description of an optical investigation of the excited state of the F center in KI using a ruby laser as an excitation source.

EXPERIMENTAL DETAIL

The experimental arrangement is shown in Fig. 1. An additively colored KI crystal (obtained from

Harshaw) containing $10^{15} \sim 10^{17}$ F centers/cm^3 was placed in a cryostat capable of cooling the sample interior to 15°K, (15°K being the limit of our thermocouple reliability). The sample size was typically 3 mm×1 cm×1.5 cm. It is very important to perform the spectroscopy on a sample that remains unchanged during the course of a particular run. The procedure adopted was to pre-expose the sample before each run to about 20 laser pulses so that a dynamic concentration equilibrium could be reached between the F and the F' centers. Under this dynamic condition, we encountered a systematic error (i.e., F bleaching) of only 1–2% throughout a complete run (involving about 200–300 shots). Repeated checks on several reference spectral points served as additional assurance that the sample remained essentially unchanged throughout each run.

A pulsed ruby laser (Trion LS4) capable of a 30-J output was used as an excitation source. A set of wire-mesh filters served as a convenient means of attenuating the laser intensity. The response of the crystal to the excitation consisted of a "fast reaction" which followed the laser intensity rather closely (within the radiative life time of F^*), and a "long term effect" which persisted after the excitation pulse. In order to separate these two effects, a mechanical chopper was added to cut off the laser light in about 50 μsec.

The auxiliary spectroscopic light sources consisted of a tungsten ribbon filament lamp (Westinghouse

† Supported in part by the National Science Foundation.
* Present address: Bell Telephone Laboratories, Murray Hill, New Jersey.
[1] F. Seitz, Rev. Mod. Phys. **26**, 7 (1954).
[2] Schulman and Compton, *Color Centers in Solids* (The Macmillan Company, New York, 1962).
[3] F. Lüty, Z. Physik **160**, 1 (1960).
[4] R. K. Swank and F. C. Brown, Phys. Rev. **130**, 34 (1963).
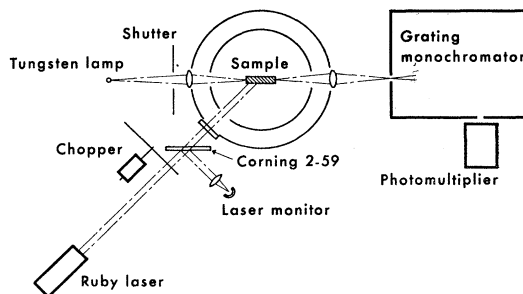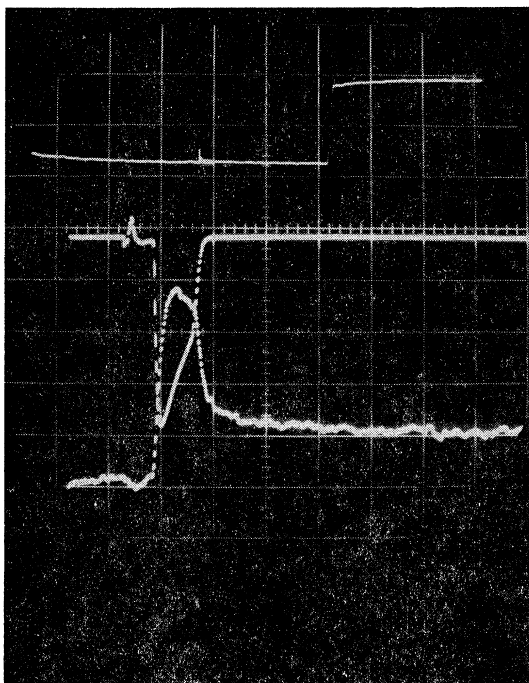
Fig. 1. Experimental apparatus for the visible region spectroscopy.

FIG. 2. A typical oscillogram, taken at 3.17 eV. Top trace, shuttered dc light (20 msec/cm); middle trace, laser monitor signal (0.5 msec/cm), bottom trace, the laser-induced change in the transmitted light. (The positive signal means an increased absorption.)

EDS, 6V at 18 A) to cover the 1- to 4-eV region, and a Perkin Elmer Globar for the 0.25- to 1-eV region. Both of these sources were connected to a storage battery string with a transistorized current regulator in series which kept the current variations within 0.1% despite the input voltage variation of 50% due to the current drain on the battery. The use of the current regulator simplified the measurement technique of the static spectrum (i.e., F ground state).

The portion of the spectrum near the 4-eV region was double checked using an 800-W xenon arc source (Hanovia Lamp Division) which improved the signal-to-noise ratio by a few orders of magnitude. However, the use of this source was limited because of the complex emission spectrum of xenon in the visible region.

The tungsten filament and xenon arc sources were focused on the front of the crystal by the quartz lens window, whereas the Globar source was focused by external mirror optics through Kodak IRTRAN windows. A mechanical shutter was placed between the window and the source in order to minimize the bleaching of F centers. Typically, the crystal was exposed for 0.1 sec duration every 2 min for the nitrogen-temperature runs and every 3 min for the helium-temperature runs. The light from the back of the crystal was focused on the entrance slit of the monochromator (Bausch & Lomb 500-mm grating monochromator for the visible region and Perkin Elmer prism monochromator for the infrared region), the output of which was

detected by photomultipliers (RCA 1P28 and RCA 7102), or a PbSe photoconductive detector (Santa Barbara Research Center) housed in a miniature dry-ice Dewar.

Figure 2 is a typical oscillogram containing information about a spectral point. The uppermost trace shows the shuttered probe light (negative signal for increasing light intensity). The brightened portion of this trace corresponds to the laser excitation, and this portion is amplified and expanded in the bottom trace. The middle trace is the output from the laser-intensity monitor in the same expanded time scale as the bottom trace.

There are several sources of inaccuracies in the present experiment which will be enumerated.

Stray light. Near the laser photon energy and the fluorescence photon energy regions, the scattered light from the Dewar enters the monochromator and swamps the light at the frequency of the monochromator setting. In principle this effect can be subtracted away, and this is done. This subtractive procedure, however, becomes difficult when the stray light exceeds the observed signal by a factor of three or more. This fact can be seen from the size of the estimated error in the spectra.

Infrared source. Both the Globar output and the infrared detector sensitivity fall off rapidly from 0.25 eV down. Thus at 0.25 eV, the transmitted light is several orders of magnitude below that at 0.5 eV. Therefore, it becomes increasingly difficult to trust the observed result.

Long-term effect. By far the greatest source of error resulted from a laser-induced long-term effect, caused by the $F \rightarrow F'$ conversions. As can be seen in the following section, the spectrum associated with this effect yields valuable information on the F' spectrum. In order to separate this effect from the laser dependent part, a mechanical chopper was added to cut off the laser. However, the finite cutoff time introduces a serious drawback in the accurate interpretation of the observed oscillograms, particularly in those spectral regions where two effects have the same sign. In a future study, it would be quite useful to utilize a Kerr shutter to insure the sharp cutoff. Coupled with a more complete understanding of electron kinetics, it is hoped that accurate quantitative data could be obtained from this type of experiment

DISCUSSION OF RESULTS

A. Electron Kinetics

As we have seen in previous sections, there are several electronic states connected by the incident photon absorption. It will be useful to understand the electron kinetics encompassing these states. Figure 3 illustrates schematically four states which are pertinent to the present discussion. The ground state labeled F has an initial concentration, N. The measurement of
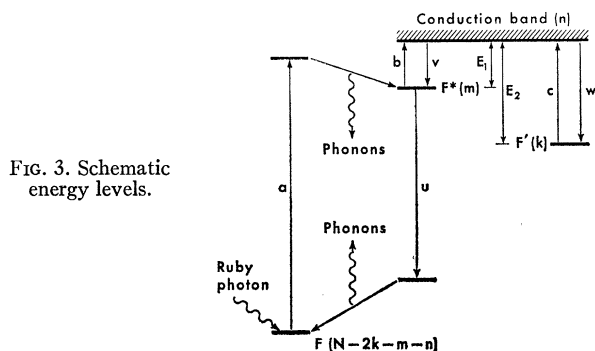
FIG. 3. Schematic energy levels.

TABLE I. Concentrations of four states at three different times.

Time	$F:N$	$F^*:m$	$F':k$	Cond. Bd:n
0	N	0	0	0
1	$N-m-n-2k$	m	k	n
2	$N-2(k+fn)$	0	$k+fn$	0

the absorption constants at predominantly F and F' spectral points before and a sufficiently long time after the laser excitation yields approximate estimates of the equilibrium concentration ratio of F' to F centers in the absence of the laser excitation. Typically this ratio is about 2% at 77°K and about 0.5% at 15°K. In order to simplify the algebra it will be assumed in the following analysis that the crystal contains no F' centers before each laser excitation. We are justified in making this assumption because we generally convert 10–50% of F centers into F' centers during the laser excitation, and therefore the initial F' concentration can be neglected.

The first excited state labeled F^* with a concentration m is an extremely important state for the present experiment, since this is the state on which we perform an optical absorption spectroscopy. In addition the fluorescence initiates from this state. At temperatures considered in this experiment m is equal to zero before and a sufficiently long time after the laser excitation.

The third state defined by the F' centers with a concentration k exists in this analysis as a result of the $F \rightarrow F'$ conversion. A creation of an F' center is accompanied by a simultaneous destruction of two F centers and a creation of a I^- vacancy or an α center.

Finally one must consider a conduction band with n free electrons. (In principle n can be observed by a photoconductivity measurement.) The conduction band is accessible from the F' state by an optical excitation.[5] The photoconductivity data on KCl by von Gericke[6] shows that E_2 is of the order of 0.42 eV. This fact coupled with the data of Pick[5] assures a negligible accessibility of the conduction band from the F' state via thermal excitation. The conduction band can also be reached from the F^* state through a thermal ionization process, as shown by Swank and Brown.[4] In order to understand the results of the present experiment, it will be necessary to include additional mechanism of an F^* ionization, as will be shown.

The lifetime of the free electron is extremely short. Swank and Brown[4] cite 10^{-8}–10^{-9} sec for F-center concentrations of 10^{15}–10^{16}/cm³. Therefore, at a sufficiently

[5] H. Pick, Ann. Physik **31**, 365 (1938).
[6] V. O. von Gericke, Nachr. Akad. Wissen., Göttingen I, (1950).

long time after the laser excitation, the free-electron concentration will vanish if the thermal excitation of F' centers does not exist which is the case in the present experiment.

As can be seen in Fig. 3, the process

(free electron)$+\alpha \rightarrow F^* \rightarrow F+$ (fluorescence)
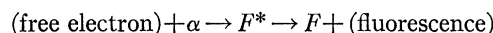
is taken in preference to

(free electron)$+\alpha \rightarrow F+$ (fluorescence).
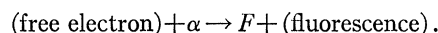
The experimental justification for this choice lies in the fact that the F-center luminescence consists of a single band rather than two separated by E_1.

Consider an idealized sequence of events which occurs in our experiment. The F center is excited by the laser light of a constant intensity for a duration of 0.4 msec, at the end of which period some new equilibrium (or quasi-equilibrium) concentrations have been reached for the states involved. Now, the laser light is cut off in zero time. The F^* electrons will decay into the F state (a temperature-independent process) accompanied by a fluorescence emission. A fraction of free electrons in the conduction band will be captured by F centers resulting in F' centers, while the rest will be trapped by α centers forming F^* centers which in turn decay into the F state.

Table I summarizes these events. Using the quantities listed in Table I, we can write absorption constants at three different times, designated by subscripts 0 (time just before the laser excitation); 1 (just before the laser cutoff); and 2 (a sufficiently long time after the laser cutoff).

$$\alpha_0 = N\sigma_F,$$
$$\alpha_1 = (N-m-n-2k)\sigma_F + m\sigma_{F^*} + k\sigma_{F'} + n\sigma_c, \qquad (1)$$
$$\alpha_2 = (N-2k-2fn)\sigma_F + (k+fn)\sigma_{F'},$$

where

$N =$ initial F-center concentration,

$m = F^*$ concentration at time 1,

$n =$ free-carrier concentration at time 1,

$k = F'$ concentration at time 1,

$f =$ fraction of free carriers trapped by F,

$\sigma_F =$ absorption cross section of F,

$\sigma_{F^*} =$ absorption cross section of F^*,

$\sigma_{F'} =$ absorption cross section of F',

$\sigma_c =$ absorption cross section of the free carriers.
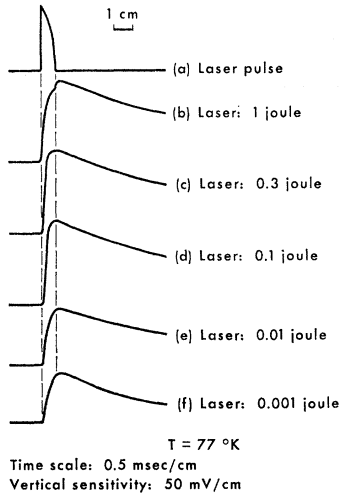
FIG. 4. Saturation behavior of $F \to F'$ conversion process as a function of the laser intensity at 1.55 eV.
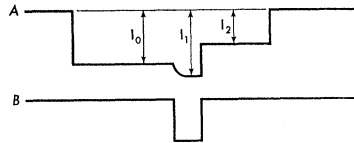
FIG. 5. An idealized oscilloscope display.
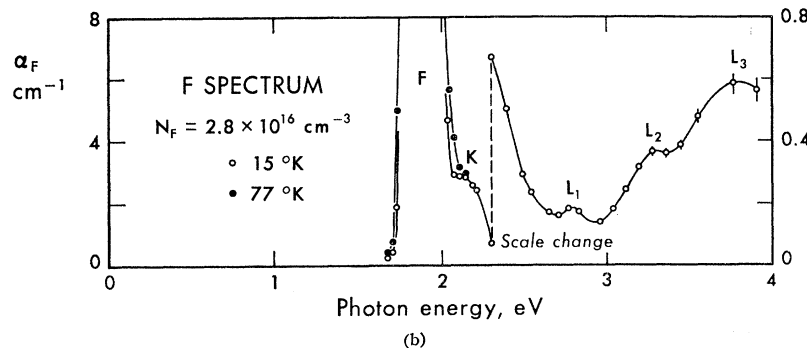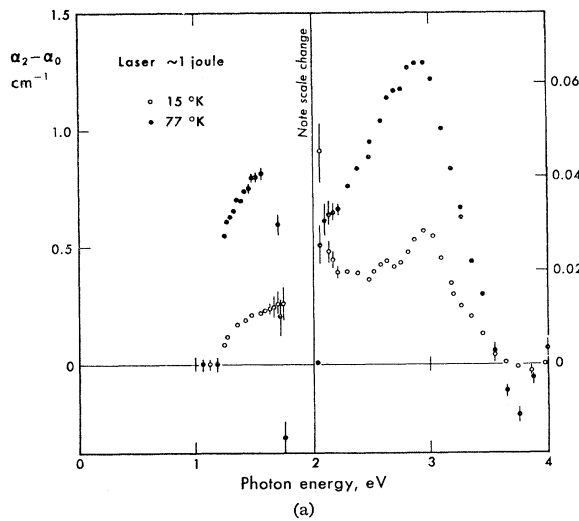
FIG. 6. (a) A typical spectrum of $(\alpha_2-\alpha_0)$, (b) The ground-state spectrum, α_F.

The contribution to α_1 from the free carriers can be neglected because their concentration is presumably small compared with others due to their short lifetime. In addition, the free-carrier absorption cross section can be shown to be small. It is clear that a simple manipulation of Eq. (1) will yield the desired optical spectrum of the F^* state as well as of the F' state. Thus,

$$\sigma_{F'} - 2\sigma_F = (\alpha_2-\alpha_0)/(k+fn),$$

$$\sigma_{F^*} - \sigma_F = (1/m)[(\alpha_1-\alpha_2)+n\sigma_F+fn(\sigma_{F'}-2\sigma_F)]. \quad (2)$$

Now, we must consider the validity of the above idealization. The laser intensity is far from constant. Not only does it have high-frequency modulations within each pulse, but also the envelope of these modulations is a shape resembling a truncated exponential decay. These two factors are, however, completely beyond our control since they are the inherent properties of the laser. Fortunately, these spikes are spaced close enough in time so that the sample is unable to resolve them. On the other hand, the envelope shape varies so slowly that we can assume safely some quasi-equilibrium concentrations for the states under consideration.

The assumption regarding the laser cutoff is much more difficult to approximate. The 50 μsec cutoff time achievable with the present chopper is much longer than all transition times. There are several reasons to believe that the present cutoff does not radically alter the qualitative results we hope to obtain. The shape of absorption spectra is certainly independent of the laser cutoff time. An important criterion of the "shortness" of the laser cutoff is the number of laser photons absorbed by the crystal during the cutoff, compared with a typical number of electrons involved in the kinetics. At 1-J laser output, the number of photons emitted during this cutoff is about 5×10^{16} with the present chopper. The absorption constant at the laser energy due to approximately 10^{16} (F' centers)/cm^3 is of the order of 1 cm^{-1}. The number of photons absorbed per cm^3 by F' centers during the cutoff is about 10^{16}. The situation in reality must be much better, however, since we must have a high rate of nonradiative reformation of F' centers. This assertion

is born out by an experimental observation illustrated in Fig. 4. It shows a set of oscilloscope traces at a predominantly F' spectral point (1.55 eV). These traces show the laser induced absorption, and therefore correspond to the F' concentration generated by the laser excitation. If there were an appreciable amount of F' bleaching during the laser cutoff, we would observe a corresponding decrease in the absorption during this period. In fact no such decrease is evident in these traces.

It can be concluded, therefore, that the idealized sequence of events assumed in the analysis can be reasonably approximated.

B. The F' Spectrum

Figure 5 is an idealized oscilloscope display consistent with the electron kinetics described in the previous section. Trace A shows the detector output with three pertinent intensities labeled; the dc probing-light intensity before the laser excitation (I_0), at the end of the laser excitation (I_1), and the intensity after the laser cutoff (I_2). Trace B is the idealized laser excitation assumed in the present analysis. Consider the "long-term effect" which is conveniently measured as

$$(I_2-I_0)/I_0=e^{(\alpha_0-\alpha_2)x}-1.$$

Therefore,

$$\alpha_0-\alpha_2=x^{-1}\ln(1+\text{"long-term effect"}).$$

But note that from Eq. (2),

$$\alpha_2-\alpha_0=(k+fn)(\sigma_{F'}-2\sigma_F). \qquad (3)$$

Figure 6(a) is a plot of $(\alpha_2-\alpha_0)$ for a representative run. In Fig. 6(b), we reproduce the measured spectrum of σ_F, in which the knowledge of Lüty's data[3] is used to draw lines through scattered points in the Lüty band region. One should be able to fit the σ_F carefully to these curves, thus obtaining a quantative estimate of $k+fn$ as well as $\sigma_{F'}$. Such an attempt results in Fig. 7. The uncertainty rising from the finite laser cutoff necessarily makes the numerical factor $k+fn$ semiquantitative at best.

Figure 4 contains a series of oscilloscope traces taken at 1.55 eV in order to illustrate the intensity dependence of the quantity $k+fn$. Notice particularly traces (c) and (d). It is clear that the quantity k reaches a steady-state value in 0.4 msec, during which the crystal is being excited, provided that the laser intensity is high enough. Furthermore, we note that k attains a saturation value already at 0.1-J laser input. In the absence of a detailed understanding of the kinetics, it is very difficult to establish from our data the dependence of $k+fn$ on the F-center concentration. The conversion process seems to be a very sensitive function of many factors including the sample size, sample-preparation technique, chopper speed, and other details of the experiment.
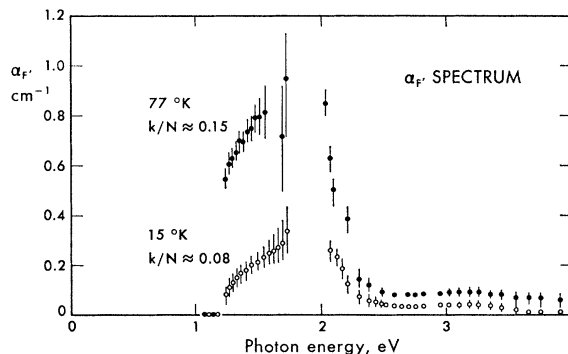
FIG. 7. Absorption spectrum of the F' center. The sample is the same as in Fig. 6(a).

C. The F^* Spectrum

An important result of Eqs. (1) and (2) is that the F^* spectrum is related to the data in a simple way, i.e.,

$$\alpha_1-\alpha_2=m(\sigma_{F^*}-\sigma_F)-n\sigma_F-fn(\sigma_{F'}-2\sigma_F). \qquad (4)$$

An experimentally convenient quantity to relate is the "short term effect" which is defined as

$$(I_1-I_2)/I_0=e^{(\alpha_0-\alpha_1)x}-e^{(\alpha_0-\alpha_2)x}.$$

The quantity $(\alpha_2-\alpha_1)$ is related to the above as follows;

$$(\alpha_2-\alpha_1)x=\ln\left(1+\frac{\text{"short-term effect"}}{1+\text{"long-term effect"}}\right).$$

Figures 8 and 9 contain the plots of $(\alpha_2-\alpha_1)$ for two representative runs. Figure 9 contains, in addition, the fluorescence intensity data in order to show the relationship between the absorption and the emission processes, which will be discussed later. Again, we should be able to fit σ_F and $(\sigma_{F'}-2\sigma_F)$, thus obtaining quantitative estimates of all the scaling factors as well
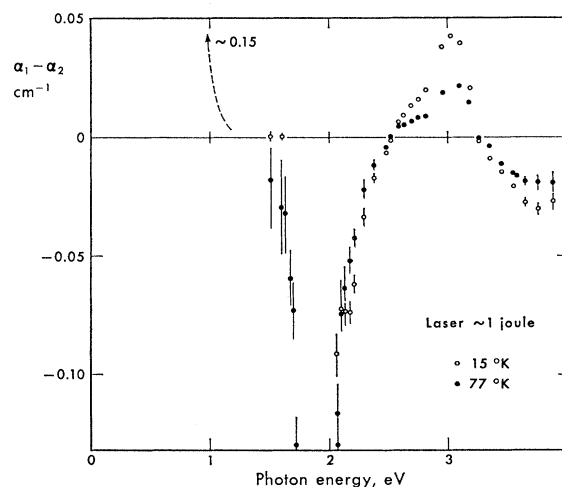
FIG. 8. A typical spectrum of $(\alpha_1-\alpha_2)$ in the visible region. The sample is the same as in Fig. 6(a).
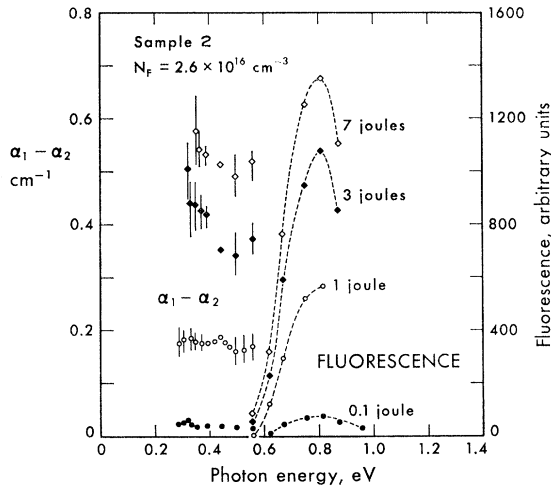
FIG. 9. A typical spectrum of $(\alpha_1-\alpha_2)$ in the infrared region.

TABLE II. Estimate of the F^* concentration from the visible region spectra.

| | $|\alpha_1-\alpha_2|$ | | α_F | | $|\alpha_1-\alpha_2|/\alpha_F$ | |
	$T=77°K$	$T=15°K$	$T=77°K$	$T=15°K$	$77°K$	$15°K$
$\hbar\omega_1$	0.019	0.022	0.267	0.247	0.07	0.09
$\hbar\omega_2$	0.0165	0.027	0.248	0.275	0.067	0.094
$\hbar\omega_3$	$\sim$0.2	$\sim$0.22	2.79	2.34	$\sim$0.07	$\sim$0.094
$\hbar\omega_4$	$\sim$0.17	$\cdots$	2.5	$\cdots$	$\sim$0.068	$\cdots$

as the spectrum σ_{F^*} itself. This multiparameter fitting process is necessarily a difficult task, and will yield uncertain quantitative results. In each of the two spectra in Fig. 6(a), there are four points at which $(\alpha_2-\alpha_0)$ vanishes (3.9, 3.58, 2.03, and 1.74 eV for 77°K; and 4.0, 3.87, 2.03, and 1.74 eV for 15°K). Hence at these energies, $(\alpha_1-\alpha_2)$ depends only on σ_F and σ_{F^*}, as can be seen from Eqs. (3) and (4). Table II lists the values of $(\alpha_1-\alpha_2)$ [from Fig. 8] and α_F [from Fig. 6(b)] at these points. The fact that the ratios of $(\alpha_1-\alpha_2)$ and α_F are essentially constant at these four energies strongly favors the possibility that there is no contribution from the visible region to the F^* spectrum. In fact, a calculation of the rest of the data points bears out this assertion provided that the scaling factor f_n in Eq. (3) is a small negative number. This seemingly nonphysical situation can be explained as follows: (1) the effect of the finite laser cutoff time, as discussed earlier, on the spectrum of $(\alpha_1-\alpha_2)$ is to cause a fraction of $(\alpha_2-\alpha_0)$ to be included in the spectrum of $(\alpha_1-\alpha_2)$, and (2) the direction of this effect (i.e., the F' bleaching during the laser cutoff) is such that the scaling factor in effect becomes negative.

An alternative to this conclusion (namely, that there is a real absorption band in the visible region, which may appear plausible particularly in view of the peak at 3 eV) results in the following difficulty. Whatever set of scaling factors we employ, the resulting F^* spectrum always contains a large residue of the F spectrum fragments. Furthermore, there occur irreconcilable discrepancies between the nitrogen and the helium temperature runs in the region of 1–2 eV. In summary, Fig. 10 shows the spectrum of the F^* absorption expressed in terms of the absorption cross section.

We make the following observations. The absorption band located in the infrared region results from a photoionization of the F^* centers. This assertion is supported by (1) the work of Swank and Brown,[4]

which shows the thermal ionization energy of the F^* to be 0.11 eV; (2) the theoretical work of Fowler,[7] who calculates the F^* wave function taking into account the electronic polarization effect, and concludes that the F^* state is a very diffused state. A drastic approximation which results from this conclusion is then to assume hydrogenic energy levels modified by the dielectric constant for the F^* state. This places the onset of the continuum band at 0.15 eV above the F^*. (3) Both the infrared absorption strength and the peak fluorescence emission depend in the same way on the laser excitation intensity, as can be seen in Fig. 9. Since the fluorescence initiates from the F^* state, we assign the same initial state to the absorption. Furthermore, since we are unable to detect any other absorption in the visible region assignable to the F^* state, we claim that this infrared absorption corresponds to the ionization of the F^* state.

Assuming that the F^* center is sufficiently localized so that we may use the Lorentz local-field model, we can estimate the oscillator strength of the F^* absorption thus far measured. This estimate yields an oscillator strength of 0.7±0.3. Because of the effective-mass approximation (which is applicable because the F^* is so diffused) we expect the oscillator strength to approach a value of about two. Therefore, there exists a reasonable promise that strong absorption and/or structures can be seen further out in the infrared region.

It is important to note that there is a strong overlap of the F^* absorption band and the ordinary fluorescence band. Due to this overlap, a pair of F^* centers will interact with and annihilate each other either via emission and reabsorption of a photon or via near-
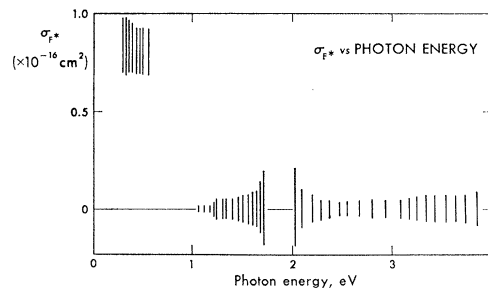
FIG. 10. Absorption spectrum of the F^* center.

[7] W. B. Fowler, Phys. Rev. 135, A1725 (1964).

zone dipole-dipole interaction,[8] resulting in the following reaction:

$$F^* + F^* \rightarrow F + \text{electron} + \text{vacancy}.$$
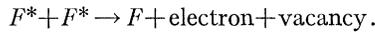
For a crystal with a characteristic dimension of 1 cm, and with an F^* concentration less than 10^{15} per cm^3, the cascade process (i.e., emission and reabsorption of a photon) should dominate the dipole-dipole process by a factor of 30. Since the cascade process depends on the sample geometry, the nonradiative reaction of the above type will be negligibly small in a crystal with a characteristic dimension much less than $0.1/\sigma_{F^*}m$. For a typical situation in our experiment ($\sigma_{F^*} \approx 10^{-16}$ cm^2, $m \approx 10^{15}$ cm^{-3}) this dimension is about 1 cm. This kind of mechanism is essential to explain the observed $F \rightarrow F'$ conversion under F-light irradiation, which should not have existed in our experiment according to the usual model of the F-center kinetics. Furthermore, this process may explain the low-temperature residual photoconductivity under F-light excitation.

The details of the electron kinetics are determined largely by what happens to those electrons that are ionized by the pair interaction suggested above. A significant experimental result is that we are unable to invert completely the populations of F and F^* centers despite the high-intensity excitation scheme used in our experiment. (At 10-J laser energy, the excitation rate is approximately 10^7 sec^{-1}, while the radiative de-excitation rate is 5×10^5 sec^{-1}.) The cascade process by itself cannot account for this phenomenon, since at best it will increase the de-excitation rate by a factor of 2. Furthermore, as pointed out earlier the laser-induced F' concentration saturates at a low value of the excitation intensity, thus making this factor of 2 even smaller in reality. Therefore, we must look for another kind of process which will depopulate the F^* states much faster than the process involving the fluorescence photons.

TABLE III. Dependence of the F^* concentration on the excitation intensity and the F-center concentration.

Sample No.	$N \times 10^{-16}$ (cm^{-3})	I (joules)	$(NI)^{1/2}$	$(\alpha_1 - \alpha_2)$ at 0.4 eV (cm^{-1})	$\dfrac{\alpha_1 - \alpha_2}{(NI)^{1/2}}$
1	0.525	1	0.725	0.084	0.118
1	0.525	3	1.26	0.151	0.120
2	2.6	1	1.61	0.176	0.108
2	2.6	3	2.80	0.382	0.135
2	2.6	7	4.27	0.515	0.121
3	1.5	0.8	1.10	0.12	0.109
3	1.5	3	2.12	0.23	0.108
4	0.6	1.2	0.85	0.10	0.118
4	0.6	4	1.55	0.20	0.129
4	0.6	6	1.90	0.22	0.116
5	5.28	1.2	2.51	0.28	0.112
5	5.28	4	4.60	0.58	0.126
5	5.28	6	5.64	0.64	0.113

Table III lists that portion of our data where the excitation rate is larger than the radiative decay rate. A close examination shows that the F^* concentration is proportional to $(NI)^{1/2}$ within experimental accuracy ($\pm 10\%$). A series of approximations to the kinetic equation of the F^* concentration results in this type of intensity and concentration dependence if we include a loss term proportional to the square of the F^* concentration. An immediate likely candidate for this loss mechanism is the dipole-dipole pair interaction mentioned earlier.[8] However, in order for this to be true, there must be a large spatial fluctuation of either the F-center concentration or the laser intensity so that this process can dominate the cascade process. The experiment of Frölich and Mahr,[9] on the other hand, shows that the F^* lifetime (measured on crystals with a similar set of parameters to ours) remains large (10^{-6} sec). The implications of this measurement are (1) our samples contain larger spatial fluctuations of F-center concentrations than their's, resulting in a strong dipole-dipole interaction in our samples; or (2) some complex difference arising from the excitation mode employed (they used a Q-switched laser); or (3) there exists some other complex mechanisms of the F^* decay which involve the electrons in the conduction band and accompanying phonons produced by the cascade process already suggested in order to explain the $F \rightarrow F'$ conversion. In the absence of detailed data pertaining to the free electrons it is very difficult to postulate the details of the kinetics. However, the examination of our data suggests that there must exist a mechanism which in the limit of high intensity excitation reduces to a simple pair-interaction picture outlined above.

CONCLUSION

The use of a high-power laser as an excitation source enabled us to use optical spectroscopy to examine the excited state of the F center. The absorption spectrum of the F^* thus obtained shows an important overlap with the ordinary fluorescence, which is necessary to explain the kinetics. When the present experiment is refined, and is supplemented by a critical measurement of photoconductivity, much knowledge will have been obtained regarding the excited state of the F center.

ACKNOWLEDGMENTS

[8] D. L. Dexter, J. Chem. Phys. 21, 836 (1953).

[9] D. Frölich and H. Mahr, Phys. Rev. Letters 14, 494 (1965).

FIG. 2. A typical oscillogram, taken at 3.17 eV. Top trace, shuttered dc light (20 msec/cm); middle trace, laser monitor signal (0.5 msec/cm), bottom trace, the laser-induced change in the transmitted light. (The positive signal means an increased absorption.)